Tellus (1990), *42A*, 140–164

On the influence of the Alps on a cold front

By KLAUS P. HOINKA, MARTIN HAGEN, HANS VOLKERT and DIETRICH HEIMANN,
DLR, Institute for Atmospheric Physics, D-8031 Oberpfaffenhofen, FRG

(Manuscript received 17 November 1988; in final form 19 May 1989)

ABSTRACT

This paper discusses the synoptic-scale environment and the scale dependent features of a cold front which crossed southern Bavaria on 8 October 1987. The analysis is based on rawinsonde, Doppler radar, aircraft and surface data. The observations reveal that the front was of the ana-type in the synoptic-scale. Its leading edge exhibited small-scale, bore-like characteristics which are typical for an atmospheric gravity current interacting with a stable layer at the ground. The leading edge was marked by several spectacular roll clouds; their generation was favoured by south-foehn in the pre-frontal area and by post-frontal precipitation. The low-level front was retarded by the Alps whereas the upper level front crossed the Alps without being distorted. The analysis shows that the cross-frontal gradients in pressure and temperature were stronger close to the Alps than at a greater distance from the obstacle. The data suggest that the middle tropospheric extrusion of cold air towards the front in a downward direction and from behind, which is a characteristic synoptic-scale feature of an ana-front, is weakened in the vicinity of the orography.

1. Introduction

Fronts cross the European Alps on about 75 days each year causing approximately 50% of the annual precipitation (Hoinka, 1985). This demonstrates the strong impact of fronts on the weather and climate of the northern Alpine region itself and the adjacent forelands of Switzerland, southern Germany and Austria. Weather forecasters in these regions face particular difficulties due to the often irregular behaviour of fronts above complex terrain. Fronts are observed to be deformed or slowed down, but they can also be intensified or are rapidly propagating along the borders of the Alps. A recent example for the latter case is discussed in Heimann and Volkert (1988). The processes that give rise to these features are not well understood.

In order to study the impact of the Alps on cold fronts, an experimental effort was undertaken, called the "German Front Experiment 1987" (Hoinka and Volkert, 1987). The main purpose of this experiment was to collect data, which resolve phenomena from the synoptic to the small scale, in order to investigate the structure and the development of orographically influenced cold fronts in the vicinity of the Alps. One of the specific questions to be addressed was to what extent cold fronts become distorted by the Alps and whether there are conditions in which this distortion is manifest as an acceleration of the cold air along the northern side of the Alps as happens, apparently, in other areas of the world, e.g., on both coasts of the United States (Mass and Albright, 1987) and in south-eastern Australia (Colquhoun et al., 1985).

In this study, we report on the event which occurred during the first intense observation period. During the late morning of 8 October 1987, a dry cold front crossed southern Bavaria. The front was documented in considerable detail by several aircraft penetrations, serial rawinsonde ascents at 90-min intervals, Doppler radar, and by a meso-scale network of surface stations, some equipped with sensitive microbarographs. A preliminary analysis, based only on a fraction of the data which were at the time available, was reported by Hoinka and Smith (1988; from now

on referred to as HS88). They addressed the question as to whether the leading edge of this front behaved as a gravity current by showing that the data then available did not reflect any characteristic of this type of flow.

An unusual aspect of the front were the well-formed roll clouds at its leading edge. Clouds of such appearances are frequently observed in connection with thunderstorm outflows. Satellite images sometimes show narrow bands of shallow clouds along the leading edge of cold fronts (see, e.g., Shapiro et al., 1985; Seitter and Muench, 1985) which are sometimes associated with deep convection. We present observations of the roll clouds and attempt to explain the related dynamics and the processes that generated the clouds in the particular event.

Cold fronts associated with a narrow cloud band at their leading edges and with gravity current characteristics of the small-scale head of the cold air were reported by Carbone (1982), Hobbs and Persson (1982) and Shapiro et al. (1985). The first two studies discussed the organization of a rainband and its deformation associated with a cold front. Shapiro et al. (1985) analysed the data of a strong dry cold front concentrating on the small-scale structure of the leading edge. Of particular importance for these frontal studies was that special observational systems were used in order to collect small-scale, high-resolution data by radar, tower and aircraft systems. The front reported in our paper is a cold front of moderate intensity which was characterized by the absence of significant precipitation, in particular, in southeastern Germany close to the Alps. It will be shown that the flow in the first 20 km behind the surface front is different from that observed further behind. The present case study is viewed as a contribution to confirm that this type of a front is not an unusual event. Therefore, one purpose of this paper is to extensively document the frontal event. This leads to an extension and in parts to a revision of the results in HS88, especially concerning the question whether the front exhibits gravity current type characteristics or not.

Another important feature of the cold front was its interaction with a pre-frontal foehn; the foehn led to a significant temperature increase in the pre-frontal air. This affects the front itself in a similar fashion to that reported from cool changes in south-east Australia where hot dry air is advected from the continent. Similar conditions occur in the lee of other mountain ranges. The southerly buster, an orographically trapped cold front that moves along the eastern side of the Australian Alps, may be influenced by foehn effects. In the Rocky Mountains the chinook is sometimes terminated by a cold front (e.g., Cook and Topil, 1952). However, in most studies only the aspects of either the chinook/foehn or of the front are studied. In the above-mentioned studies of frontal events (Carbone, 1982; Hobbs and Persson, 1982; Shapiro et al., 1985; Seitter and Muench, 1985) the aspect of orographic influences were only a side aspect, if considered at all. The second, and in our view, main focus of our paper is to discuss the complex interaction of foehn and front and to place special emphasis on the impact that the Alps exerted on the front in this particular case.

In a recent review of theoretical and observational studies relating to the low-level structure of cold fronts, Smith and Reeder (1988) discuss the variety of conceptual models of fronts. The recognition of the quite different appearance of the front when analysed in the synoptic-, meso-, and small-scale, respectively, leads to the necessity of defining what we mean by the term *front*. We believe that the following definition contains most of the commonly used scale-dependent aspects. A *front* is a three-dimensional transition zone between different synoptic-scale air masses, which is characterized by a significant change in meteorological parameters (e.g., temperature, potential temperature, wind). Within this zone, inclined surfaces exist (*frontal surfaces*) on which the parameters themselves are constant or on which their spatial derivatives satisfy extremal conditions (e.g., vorticity maximum). Intersections of frontal surfaces with horizontal planes in the z-, p-, θ-system of co-ordinates are called *frontal lines* and the intersections with the earth's surface are referred to as *surface front lines*.

The plan of the paper is as follows: in Section 2, a brief summary of the observational systems is given; in Section 3, the synoptic-scale environment over Europe on 8 October 1987 is described. Section 4 contains the bulk of the observations proceeding from the synoptic down to the small scale. Section 5 is devoted to a

summary of the observational evidence and a discussion of the relevant physical processes.

2. The measurement systems

During the German Front Experiment 1987 (Hoinka and Volkert, 1987), intense observations were performed in central Europe, in particular in southern Germany. For the present study, only a fraction of the entire data set obtained during the experiment is used. All locations which are referred to in the following are shown in Fig. 1. The entire area measures 370 km × 150 km. The observations for this study were made with a variety of observing systems. Surface pressure, temperature and wind velocity were recorded in Garching (University of Munich), Oberpfaffenhofen and Thalreit (both DLR), Wielenbach and Uffing (both University of Munich). The sampling rate of the pressure data was 1 min. Rawinsonde observations were provided by the German Weather Service at Munich and at Thalreit by DLR. Close to Munich at Garching, a tower of 50 m height provided measurements of temperature and wind velocity at 6 levels (1, 2, 5, 10, 20 and 50 m) with a sampling rate of 30 s.

A powered aircraft (type: Queenair) and two powered glider made data gathering flights across and parallel to the front (Fig. 1) providing measurements of pressure, temperature and moisture at a frequency of 1 Hz. Depending on the true ground speed the data are representative of a horizontal distance of approximately 50 m (Queenair) and 30 m (powered glider). For the airborne measurement systems the absolute accuracy of temperature is 0.3 K, of dew-point 1.0 K and of pressure 0.25 hPa; the relative errors are 0.1 K, 0.05 K and 0.25 hPa, respectively (for more details cf. Hoinka et al., 1988).

Radar data were obtained by a polarimetric Doppler radar located at Oberpfaffenhofen (DLR). The technical system is described elsewhere (Schroth et al., 1988). The radar operates within the C-band, and is able to measure both clear air echoes and cloud structures. During the present case, it was possible to evaluate Doppler velocities using clear air echoes within a horizontal range of up to 25 km. The absolute accuracy of the Doppler velocities depends on the signal to noise ratio, i.e., the reflectivity of the scattering particles, which is weak for clear air echoes. In this case, the accuracy of the evaluated Doppler velocities is between 1.0 and 1.5 m s^{-1}.

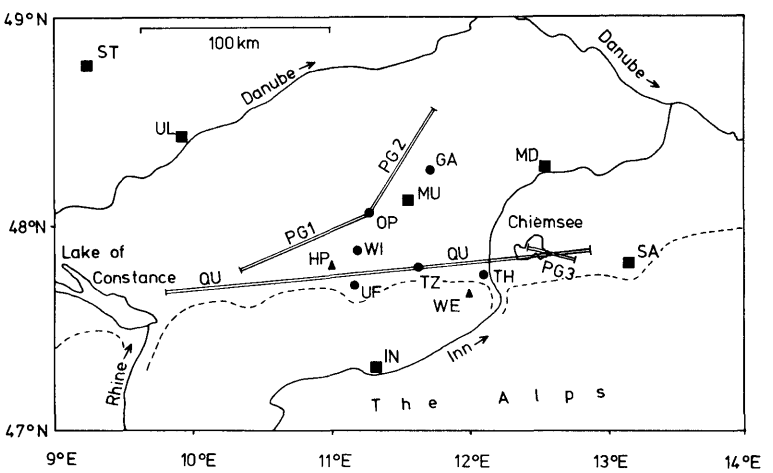

Fig. 1. Locations mentioned in the text. Synoptic stations (■): Innsbruck (IN), Mühldorf (MD), Munich (MU), Salzburg (SA), Stuttgart (ST), Ulm (UL); mountain stations (▲): Hohenpeißenberg (HP), Wendelstein (WE); other places (●): Garching (GA), Oberpfaffenhofen (OP), Thalreit (TH), Uffing (UF), Bad Tölz (TZ), Wielenbach (WI). The flight tracks of the Queenair (QU) and of two powered gliders (PG1, PG2, PG3) are indicated by double lines; the Alpine baseline is dashed. Additionally two lakes are indicated: Lake of Constance and Chiemsee. The position of the area within Europe is given in Fig. 3.

In order to remove ground-clutter a filter is applied as proposed by Passarelli et al. (1981).

During the measurements, PPI-scans (Plan Position Indicator) and RHI-scans (Range Height Indicator) were performed. The averaged data spacing for all radar scans was 300 m in range; for PPI-scans the resolution in azimuth was about 1°; for RHI-scans the elevation step was 0.3° at low elevations increasing to 2° at high elevations. In order to determine a vertical profile of wind data above the radar, VAD analyses (Velocity Azimuth Display) are performed following Browning and Wexler (1968).

For the VAD analysis, a PPI-scan at 20° elevation is used for all heights. The VAD technique is simplified to retrieve only the horizontal wind components which in turn reduces the error in areas with poor data coverage. This is done due to the magnitude of the accuracy of the Doppler velocity which is derived from measurements of clear air echoes. Within areas with precipitation a complete VAD analysis was performed on volume scans in order to estimate divergences and hence to obtain vertical velocities.

3. The synoptic-scale environment

During the period 5–9 October 1987, the synoptic-scale circulation over Europe was governed by an upper level low near Iceland. On its southern flank, short-wave troughs moved eastward and led to intrusions of cool maritime air over the continent. A first cold front terminated the period of late summer weather as it crossed central Europe early on 7 October. At this time a new depression had rapidly developed over the eastern Atlantic Ocean. This cyclone moved, still intensifying, towards the northeast and reached a position near the Hebrides at 06 GMT on 8 October with a central pressure below 965 hPa. The synoptic situation at the 850 and 500 hPa levels on 8 October, 00 GMT is depicted in Fig. 2.

The frontal system was already occluded north of 50° latitude at 850 hPa. The air masses involved are characterized by the following equivalent potential temperatures (dashed isolines): pre-warm-frontal air ($\theta_e \approx 40$°C), warm sector air ($\theta_e \approx 45$°C) and post-cold-frontal air

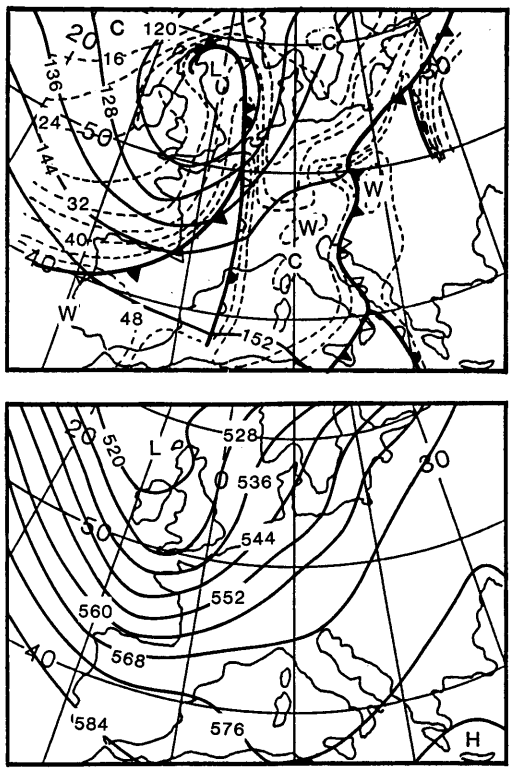

Fig. 2. Synoptic charts on 8 October 1987, 00 GMT for the levels 850 hPa (top) and 500 hPa (bottom). Solid lines designate geopotential height (gpdam), dashed lines equivalent potential temperature (°C).

($\theta_e < 30$°C). During the subsequent 24 h, the low moved towards 2°E, 63°N. The frontal system crossed central Europe entirely. At the 500 hPa level, a well-pronounced trough extended from the British Isles to the Iberian Peninsula. The trough line coincided with a zone of numerous showers. 24 h later, this trough had moved eastwards and extended from the North Sea across the Alps to the Mediterranean Sea.

The cold front passed the line Brussels–Paris–Bordeaux close to 00 GMT on 8 October. North of the Alps, it caught the preceding warm-front, but kept its cold front character. The Rhine River was crossed by 06 GMT on 8 October. At this time, moderate rain was observed near the front and an intense activity of showers was observed several hundred kilometers west of it, associated with the leading edge of the upper

level trough. During the following hours, the frontal precipitation diminished. The surface front, however, kept on moving eastward, and rapidly crossed southern Germany (Munich, 11 GMT) and eastern Austria (Vienna, 17 GMT) almost without precipitation. The upper level trough lagged behind and crossed southern Germany during the evening hours, producing rain showers and thunderstorms.

Fig. 3 shows three-hourly isochrones of the surface front line as it crossed Europe. The synoptic-scale analysis reveals that the eastward movement of the front is significantly retarded by the Alps with blocking at the western edge and a gradual encircling of the barrier at low levels. However, at higher levels the front crossed the Alps without such evident modifications. This is revealed by the infrared satellite images (METEOSAT and NOAA-9) taken around noon, which display an undistorted arc of cirrus and altocumulus clouds extending from southern Sweden across the Alps towards the Strait of Gibraltar (not shown). A sequence of 30 METEOSAT images between 7 October (18 GMT) and 8 October (18 GMT) is given in Zwatz-Meise and Kress (1988). Their analysis indicates that the mid-tropospheric front, characterized by a ridge in the field of the so-called thermal front parameter, crosses the Alps without being distorted. This parameter is evaluated from

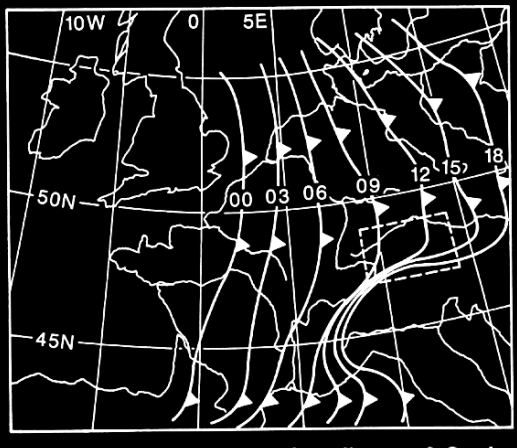

Fig. 3. Isochrones of surface front lines on 8 October 1987 (GMT) over central Europe (by courtesy of M. Kurz). The area bounded by the broken line is enlarged in Fig. 1.

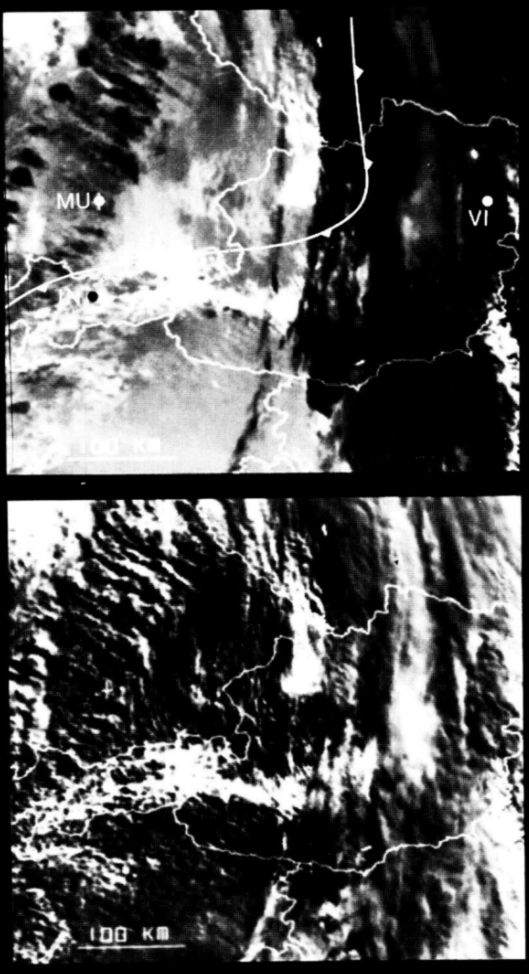

Fig. 4. NOAA-9-images from 8 October 1987, 1414 GMT: infrared (top) and visible (bottom). The abbreviations stand for: Innsbruck (IN), Munich (MU) and Vienna (VI). The black lines indicate the borders between Austria, Italy, Germany, Czechoslovakia and Yugoslavia.

the horizontal gradients of the mean temperatures taken from the layer between 500 hPa and 850 hPa (Zwatz-Meise, 1987; p. 166).

In Fig. 4, an enlarged part of the NOAA-9 image (1414 GMT) is given showing southern Germany, Austria and northern Italy. The low-level clouds cover the entire Alps (visible image; Fig. 4, bottom) and do not show a frontal zone, which is evident in the infrared image (Fig. 4, top). A narrow cloud gap, which is apparent

north of the Alpine ridge line to the east of Innsbruck, is presumably due to the south-foehn. At 1414 GMT, the surface front line was east of Salzburg in the Alpine foreland but lagged behind over the Alps (Fig. 3), paralleling the northern edge of the cloud gap. Hence, Innsbruck was still in the pre-frontal foehn area. South of the Alps in northern Italy clouds appear due to uplifting in the blocked southerly flow, which forms a foehn-wall above the Alpine ridge.

4. Scale-dependent appearance of the front

In this section, we document the scale dependent appearance of the front as reflected by the different observation systems. Phenomena of size greater than 250 km are termed *synoptic-scale*; features with typical length scales between 250 and 25 km or below 25 km are referred to as of *meso-scale* or *small-scale* extent, respectively. The scale subdivision into synoptic-, meso- and small-scale is similar to Orlanski (1975) who called these scales meso-α, meso-β and meso-γ. The threshold values of such a rank order are, of course, somewhat arbitrary, but most of the observation systems used obtained data only in one of the mentioned scales. So, a clear distinction is important when interpreting the results.

4.1. Synoptic-scale

Time–height cross-sections of serial rawinsonde ascents over a period of more than, say, 10 h give synoptic-scale patterns when a space–time conversion ($\Delta x = c\Delta t$) is applied by means of a uniform disturbance speed. This speed was computed by a least square fit analysis of the passage times taken from pressure traces in southern Germany between Ulm and Salzburg (Fig. 1). With this analysis, we obtained a velocity which represents the average over the chosen area. This was done because pressure data were available for most of the stations and the frontal signal was clearest in the pressure traces. With the assumption of a straight front line, the meso-scale analysis yields a uniform propagation speed of the surface front line of 18.1 ± 0.7 m s^{-1} towards $98° \pm 5°$, i.e., the front lies parallel to an axis from 8° to 188°. Local values of the frontal speed and of its orientation may differ from these averaged values representative for southern Germany. See

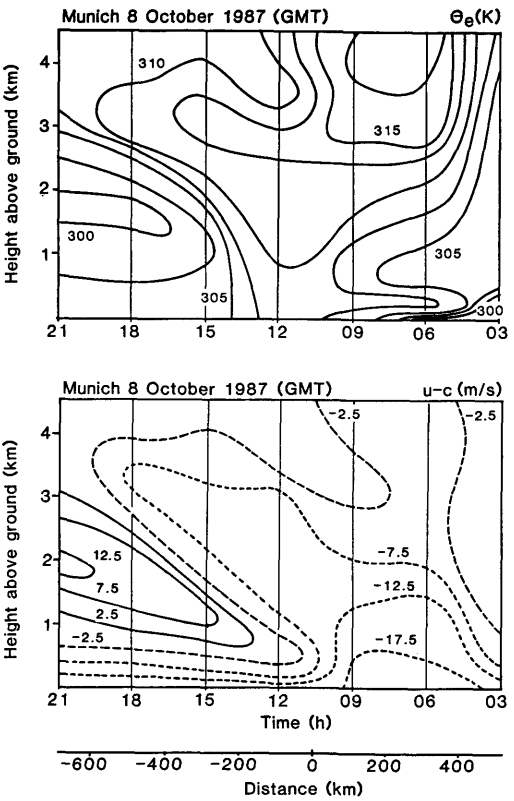

Fig. 5. Time–height cross-section from Munich rawinsonde soundings on 8 October 1987 of equivalent potential temperature (top) and relative cross-front wind component (bottom); uniform speed of the front: $c = 18.1$ m s^{-1} towards 98°.

Fig. 4 of HS88 for the geographical distribution of the pressure stations and isochrones of the frontal positions.

From the soundings of Munich, the fields of equivalent potential temperature (θ_e) and relative cross-frontal airflow (u–c) are displayed in Fig. 5 using such a frame of reference. The isolines of relative airflow had to be relabelled since first published in HS88, where c was given as only 15.5 m s^{-1} due to an evaluation error. The front is defined by a gradient zone in θ_e, which bends backwards with height. Over a distance of 200 km θ_e decreases by more than 7 K. The colder air mass seems to come from aloft in a tongue with its axis along the maximum relative flow ("feeder flow"). The structure of the isotachs of the wind suggests a descending flow in this

tongue; this is corroborated by an estimate of subsidence of about -0.04 m s^{-1} at the level of maximum flow towards the front (1420 GMT; calculated via VAD divergences from Doppler radar data). Below about 1 km, the relative flow is everywhere negative. We note that the airflow pattern in the post-frontal regime is remarkably similar to that presented for an ana-front by Bergeron (see Chromow, 1940, Fig. 126) and to the observations discussed by Browning and Harrold (1970).

East of the frontal transition zone, a marked inversion is observed close to the ground. In the pre-frontal area a south-foehn was observed. Frequently such foehn flows do not touch the ground some distance off the Alpine baseline (e.g., in Munich) because the warm air is not able to completely remove the pre-existing cold air and glides up on a shallow surface-based cold layer (Hoinka and Rösler, 1987). This layer is topped by a strong inversion separating the cold air from the warm foehnic air aloft. The inversion is apparent in Fig. 5 (top) for times prior to 09 GMT between 0 and 400 m AGL.

Fig. 6 shows the relative flow components normal and parallel to the front, which are obtained from VAD radar data sampled every 30 min in Oberpfaffenhofen during the period 08 to 18 GMT. The frontal discontinuity at 1020 GMT stands out and the previously discussed, elevated zone of positive relative flow is of similar magnitude as in the rawinsonde data, although the speed values obtained by the rawinsonde (u–c <12.5 m s^{-1}) differ from those obtained by the radar (u–c between 5 and 10 m s^{-1}). In the radar data, there are two minima in the (u–c) field not apparent in the rawinsonde data: between 09 and 10 GMT (-25 m s^{-1}) close to the ground and at 12 GMT (-20 m s^{-1}) at a height of 3.5 km. They appear because the radar is able to collect data in a denser time spacing than the rawinsonde. For the same reason, the region of positive relative flow is more pronounced in the VAD data; behind the front, it bends down to 400 m above ground. The along-front component is nearly everywhere positive with a gradual increase with height as the dominating feature in the post-frontal region; it is only close to the surface front line that a small region of negative values appears.

In summary, moderate winds came from the south prior to the passage of the front, while they changed to a westerly direction and increased in strength afterwards. During the afternoon the upper boundary of the zone of westerlies rose from 2 km to 3 km above ground; at higher levels the winds backed towards the south-west.

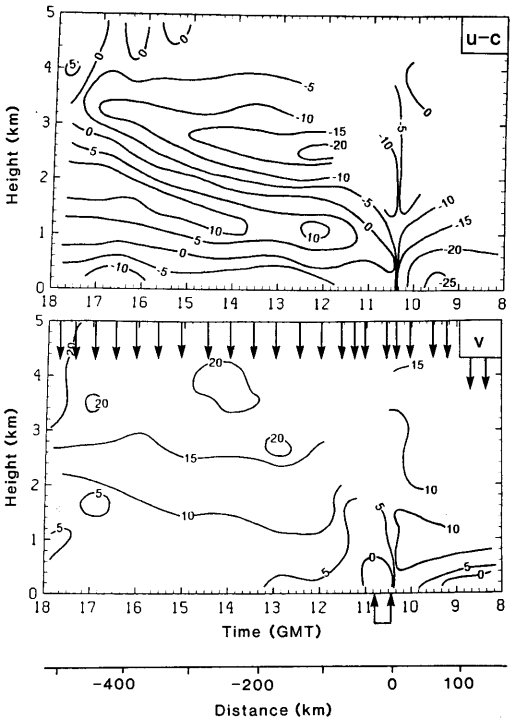

Fig. 6. Time–height cross-section of radar deduced wind relative to the front above Oberpfaffenhofen on 8 October 1987: cross-front component (top) and along-front component (bottom); uniform speed of the front: $c = 18.1$ m s^{-1} towards 98°; height in km above ground. The arrows at the upper edge indicate when the VAD profiles were computed. The two arrows at the lower edge mark the area shown in Fig. 13.

In Fig. 7, we compare time–height cross-sections from soundings of two stations at the Alpine baseline: Hohenpeißenberg (on top of a foothill, 977 m MSL) and Thalreit (on the Inn River, 454 m MSL). The frontal structure, as reflected by θ_e, is similar to the one observed above Munich (Fig. 5). In Thalreit, the inversion prior to the front is even stronger than in Munich. Hohenpeißenberg lies above the inver-

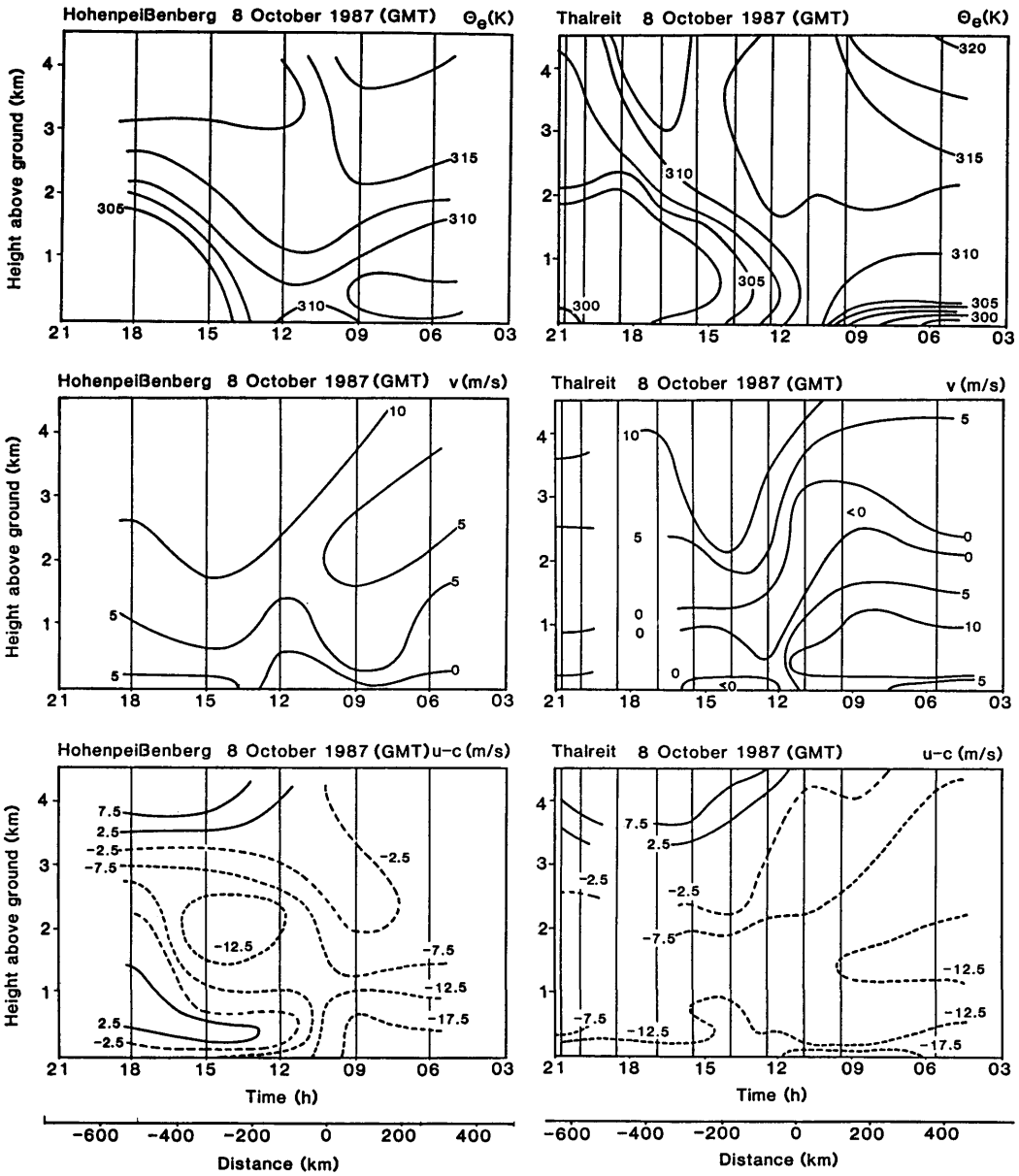

Fig. 7. Time–height cross-sections from rawinsonde soundings at Hohenpeißenberg (left) and Thalreit (right) on 8 October 1987: equivalent potential temperature (top), along-front wind component (bottom), relative cross-front wind component (middle); uniform speed of the front: $c = 18.1$ m s^{-1} towards 98°.

sion. The corresponding meridional velocity fields show everywhere a positive southerly component due to the foehn. Prior to the front, a quite strong southerly component up to 10 m s^{-1} was observed above Thalreit in a shallow layer below 1 km above ground; it can be explained as a strengthened foehnic outflow from the great valley of the Inn River.

Less consistent are the fields of relative cross-frontal velocity. The zone with positive (u–c) aloft is smaller above Hohenpeißenberg and the magnitude of the flow is weaker. At Thalreit no elevated "feeder flow" is evident. The post-frontal situation in Thalreit is complicated for two reasons, namely (a) the data gap in the wind for the period between 1530 and 1930 GMT and (b) its location close to the Alpine ridge where a great Alpine valley enters the plain. Additional evidence is available through wind registrations from Thalreit ground station (454 m MSL) and from the nearby summit of Wendelstein (1838 m MSL). At the ground, the wind was westerly and less than 7 m s^{-1} (u–$c < -11$ m s^{-1}), while at Wendelstein u–c increased with time from -8 m s^{-1} to about 0 m s^{-1}. So at those levels some relicts of the positive, relative "feeder flow" could have been present. On the other hand, the absence of the "feeder flow" towards the front above Thalreit may be explained by a deceleration due to diffluence, if parts of a westerly surge of cold air along the Alps enter the valley and move towards the south. However, this may have influence only at the low-level flow.

In order to display the orographic impact, the relative cross-front flow (u–c) is given in Fig. 8 along a cross-section perpendicular to the Alps. We are looking towards the approaching front with south to the left and north to the right. The soundings from Thalreit, Hohenpeißenberg and Munich are composited to represent the lower troposphere at increasing northward distances from the Alpine baseline: 3, 21 and 55 km, respectively. The surface front passed Hohenpeißenberg at 1008 GMT, Munich at 1040 GMT and Thalreit at 1115 GMT. The corresponding soundings are compared 4 h behind the surface front. It is evident that the depth of the "feeder-flow" decreased with decreasing distance from the Alpine ridge and vanished in the vicinity of the orography.

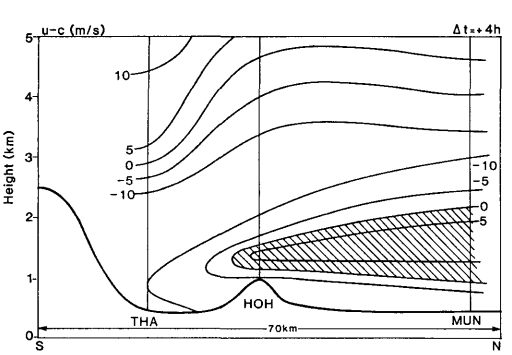

Fig. 8. Relative cross-front wind component in a cross-section perpendicular to the Alps 4 h after the passage of the surface front composited of the soundings of Thalreit (THA), Hohenpeißenberg (HOH) and Munich (MUN). The view is towards the front with south to the left and north to the right. The hatched area indicates an eastward relative flow u–c (towards the reader).

4.2. Meso-scale

Three aircraft and a Doppler radar in its 200 km range surveillance mode were the tools for examining the meso-scale features of the front. The location of the flight tracks is given in Fig. 1. The Queenair flew from east to west parallel to the Alpine baseline approximately 700 m above ground. The traces of potential temperature and relative humidity along this track are displayed in Fig. 9 (bottom). The front separated the cold air region to the left (towards the west) from the warm foehnic area to the right. When the front was crossed near Bad Tölz, the potential temperature dropped by 5 K and continued to gradually decrease by another 5 K, whereas relative humidity jumped from very dry, foehnic values (30%) to high post-frontal ones (90%).

The two powered gliders (PG1 and PG2) made data-gathering flights at a height of 1100 MSL over a distance of 150 km from the baseline of the Alps towards the northeast (Fig. 9, top). The cold air region lies to left of the indicated front, the foehnic area to its right. The warm air in the area with foehn exhibited a potential temperature of 298 K and a relative humidity of 40%. When the aircraft descended into the cold air through the leading edge of the front at 30 km north of the baseline of the Alps, the potential temperature dropped by about 6 K and the relative humidity increased to 90%. At the leading edge of the front a wave structure is apparent. With increasing distance to the north-east away from the front the potential temperature decreased from foehnic values of 299 K to 295 K; further to the north it increased again to 297 K. This may be due to the fact that during south-foehn the low tropospheric lee-side atmosphere is disturbed by the barrier; usually a meso-scale wave is forced by the moun-

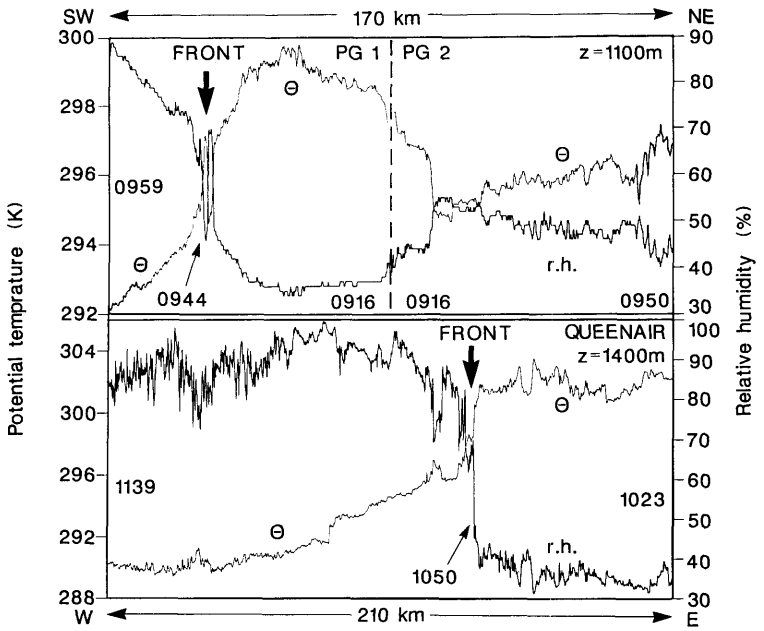

Fig. 9. Traces of potential temperature (θ; light lines) and relative humidity (r.h.; bold lines) along the aircraft traverses (cf. Fig. 1) of powered glider PG1 (top, left) and PG2 (top, right) and Queenair (bottom); the height z is given in m above mean sea level; times are in GMT.

tain with the salient feature of a deep trough just in its lee. Further to the north there is an updraught region leading to decreasing potential temperatures along a horizontal cross-section normal to the barrier.

The frontal lines defined by strong gradients in potential temperature and in relative humidity at the height 1100 and 1400 MSL are clearly depicted in Fig. 9. The horizontal extension of these frontal lines amounts to about 1 km taking into account an average aircraft speed of 30 m s^{-1}. Over this distance the potential temperatures dropped by about 2.5 K (Queenair) and by 2.1 K (PG1). The scale of these frontal lines is clearly different to that determined by the rawinsonde and radar VAD profiles.

The data discussed so far (rawinsondes, VAD radar winds, airborne systems) are all "one-dimensional". Only compositing into time–height cross-sections gave two-dimensional results. Surveillance scans by radar, however, provide us with quasi-instantaneous information from a two dimensional area of meso-scale extent. The radar reflectivity patterns at 6 times between 0913 and 1133 GMT are displayed in Fig. 10. For areas with a reflectivity larger than 20 dBZ (within the blacked spots) there was a high probability of precipitation, whereas non-precipitating clouds could have been present in the hatched areas with reflectivities between 6 and 20 dBZ. Note that the height of the scanned cloud portions increases with the distance from the radar: 1400 m at 50 km; 3200 m at 100 km; and 5200 m at 150 km.

Three important insights can be gained from Fig. 10: (a) a cloud complex moved from west to east; (b) regions with high reflectivity were restricted to the north-west sector outside of the 50 km range and they gradually dissolved; (c) the previously coherent reflectivity patterns separated into two parts after 1003 GMT. The leading portion travelled on an eastbound path and exhibited elongated ends which remain visible for more than 1 h.

The positions of the objectively analysed, uniformly moving surface front line (see Subsection 4.1) are marked in Fig. 10. For the first 3 times, the front line coincided with the easternmost

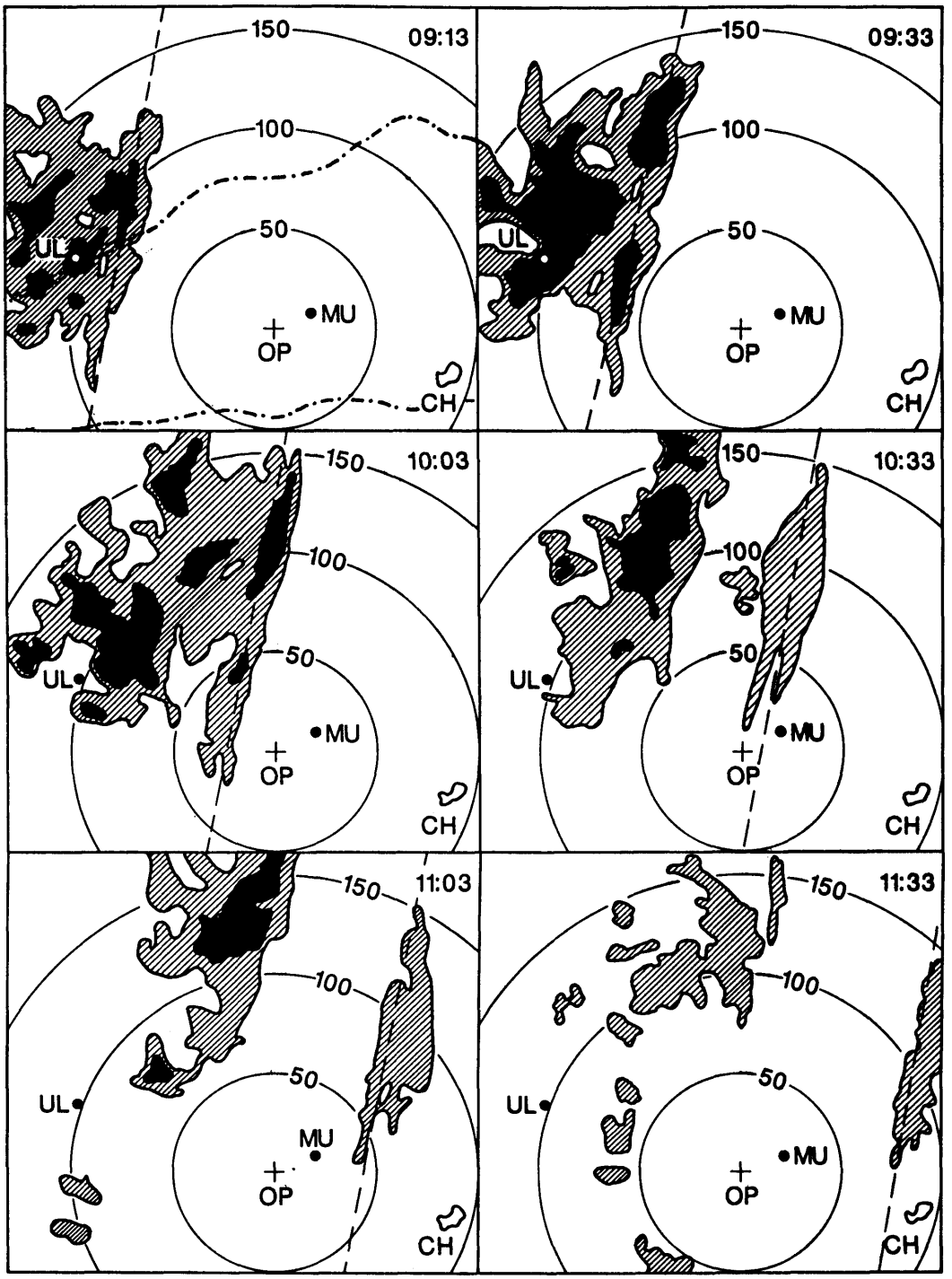

Fig. 10. Reflectivity patterns from PPI scans conducted by the Doppler radar at Oberpfaffenhofen (OP) on 8 October 1987 at the times (GMT) indicated; reflectivity >6 dBZ in hatched areas and >20 dBZ in blacked areas; range rings every 50 km; elevation of radar beam: 1.5°. The broken lines indicate the respective position of the surface front line. Locations: Ulm (UL), Munich (MU), Chiemsee (CH) and Oberpfaffenhofen (OP). In the top left frame the Danube River and the baseline of the Alps are indicated by dashed–dotted lines.

Fig. 11. First and second roll of clouds as seen from Oberpfaffenhofen on 8 October 1987, 1025 GMT. View is towards 340° (photograph by D. Heimann).

reflectivity maximum; later on it had the same orientation as the axis of the travelling, elongated cloud structure.

As meso-scale evidence, we keep in mind that a distinct difference in pre- and post-frontal air mass characteristics was determined by aircraft traverses and that the front apparently underwent a transition from a precipitating system into a dry disturbance in the area bounded by the Alpine baseline in the south and by approximately the Danube River in the west and in the north.

4.3. Small-scale

Visual observations (photographs), Doppler mode radar scans in the 40 km range, high resolution time series of meteorological parameters at different places, and 1 Hz aircraft data in the vicinity of the disturbance are used to investigate the small-scale appearance of the front.

4.3.1. Radar observations. In the eastern part of southern Germany, the most impressive visible aspect of the front were up to three roll clouds at its leading edge. Fig. 11 shows the first roll a few minutes before it passed Oberpfaffenhofen. It moved at a height of between 500 and 1000 m above ground and extended from horizon to horizon. The radar at the top of the roof scanned the clouds; the succeeding rolls can be recognized underneath the lower edge of the leading one. In a radar picture taken 10 min earlier the central portion of the three rolls is clearly visible in the velocity distribution (Fig. 12), which show three stripes of maximum velocities of more than 18 m s^{-1} towards the radar. In between of these the velocities drop down to about 8 m s^{-1}.

A quantitative composite of two cross-sections normal to the rolls is shown in Fig. 13. The left portion depicts the situation towards the rolls 2 min before the leading edge passed the radar, the right portion gives a "backside view" 14 min later. In order to evaluate the translation speed of

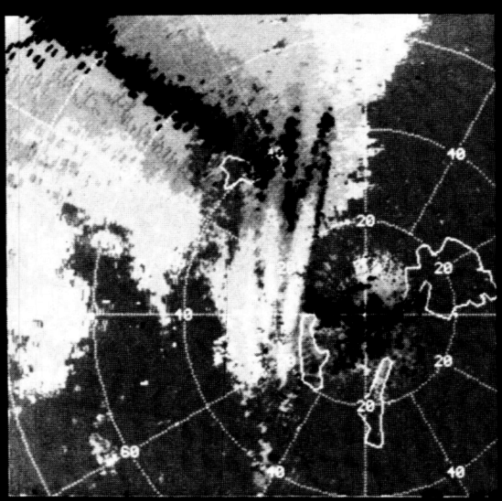

Fig. 12. Radar PPI of Doppler-velocities using an elevation angle of 2° from Oberpfaffenhofen on 8 October 1987, 1013 GMT: The city boundaries of Munich are indicated at about 20 km to the northeast. The numbers at the circles indicate the distance from the radar in km.

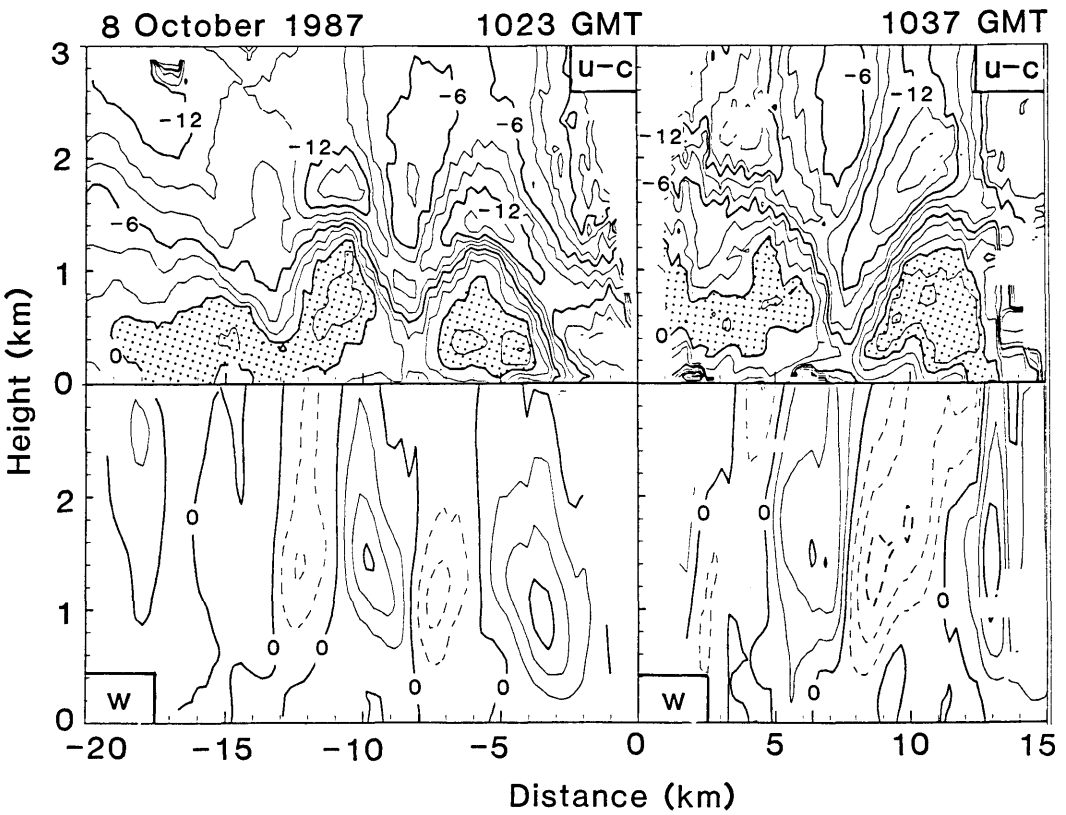

Fig. 13. Vertical cross-sections of relative flow components as measured from Oberpfaffenhofen (0 km) towards 280° (left) at 1023 GMT and towards 100° (right) at 1037 GMT on 8 October 1987: cross-front component $u–c$ (top) and vertical component w (bottom); $c = 18.1$ m s^{-1}. The isoline increment is 2 m s^{-1}. The areas with $u–c > 0$ are dotted; negative w contours are dashed.

the rolls, we compare in both cross-sections the region with the strongest gradients at the leading edge because the gradients are independent of the absolute magnitude of the wind velocity. To avoid ground clutter influences which are different in both directions, the fields at 400 m above ground are considered. The propagation speed results to 19.5 ± 0.5 m s^{-1}; the error is due to the range gate size of the radar data. Taking into account that this value represents the local measure of frontal speed, one can say that the value agrees well with the independent data from the onset of pressure jumps at 15 stations (mean value for southern Germany: 18.1 ± 0.7 m s^{-1}) and from photographic documentation at Oberpfaffenhofen and above Chiemsee (19.5 ± 1.0 m s^{-1}).

The small-scale velocity structures in Fig. 13 show a positive relative flow towards the front (maximum: 4 m s^{-1}) and three regions with gradually diminishing updraughts (maximum: 7 m s^{-1}). In the cross-front relative wind component we find, furthermore, an undulating belt of wind shear ahead and above the maxima with values up to 0.01 s^{-1} (for $\partial u/\partial x$) and 0.03 s^{-1} (for $\partial u/\partial z$). The prominent feature of positive relative flow towards the leading edge from behind reminds us of the analogy between gravity currents in the laboratory and gust lines in the atmosphere as first described by Schmidt (1911). The alternating patterns (positive and negative horizontal relative flow, updraughts and downdraughts) resemble to a high degree observations made for atmospheric undular bores, e.g., the "morning glory" in northern Australia (Smith and Morton, 1984).

Note that in contrast to laboratory gravity currents the flow towards the leading edge vanishes in the lowest 50 m. The absolute values of the flow in the lowest 100 m might be biased by not sufficiently removed ground clutter. However, the data at a height of 50 m above Garching (Fig. 14) show that the wind velocities were between 10 and 12 m s^{-1} behind the leading edge of the front. These data corroborate the estimates obtained by the radar indicating that ground clutter has not significantly biased the radar measurements. The vanishing flow towards the leading edge at low level is possibly due to frictional effects in the boundary layer which is suggested also by the decrease in wind velocity down to 7 m s^{-1} at 10 m height above Garching.

The comparison of both cross-sections separated in time by 14 min shows that the general features, e.g., spatial extent and maximum values of flow components within the rolls, remained constant. In order to estimate the grade of stationarity, it is necessary to discuss the error estimates of the evaluated wind fields. For the present case the errors in the velocity u due to the signal to noise ratio is in the order of 1.0–1.5 m s^{-1} (Section 2). To calculate vertical velocities (bottom part of Fig. 13) from data of a single Doppler radar two approximations must be made: (a) the airflow has negligible divergence and (b) along-front derivatives are small compared to the other terms. The equation of continuity is integrated upwards with $w = 0$ at the surface as a boundary condition. Assuming a convergence zone of 2 km in width, the maximum convergence error is of the order of 10^{-3} s^{-1}, resulting in an estimated maximum error in w of about 1 m s^{-1} at a height of 1000 m. A further error source is that the observed $\partial v/\partial y$ are not vanishing; if they are in the range of 1 m s^{-1} per 10 km an error range of about 0.1 m s^{-1} for w at a height of 1000 m must be expected. Taking into account these uncertainties, it is suggested that

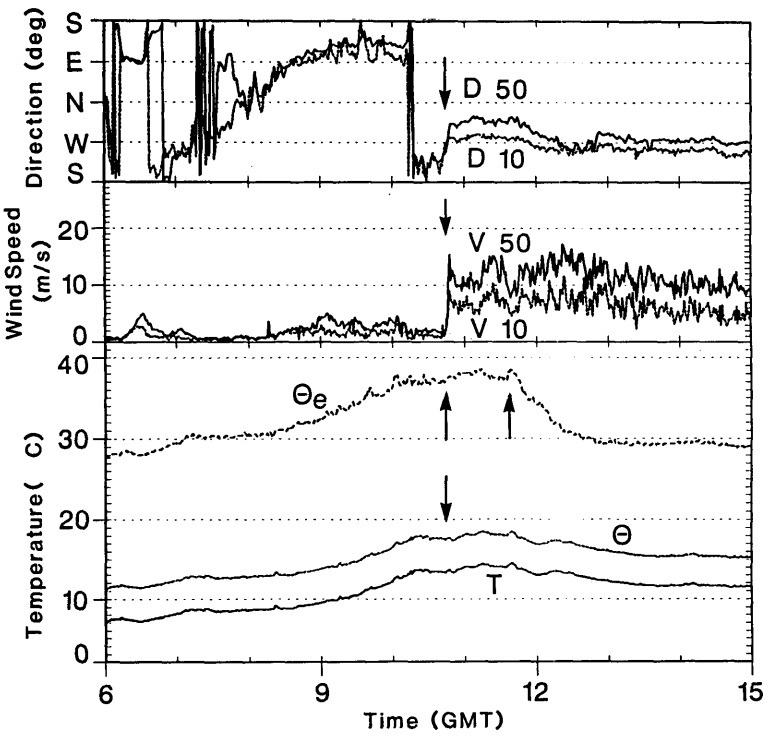

Fig. 14. Time series recorded at Garching on 8 October 1987 from 06 to 15 GMT with a measuring interval of 30 s. The symbols stand for (from top to bottom): wind direction at 10 and 50 m (D_{10} and D_{50}); wind speed at 10 and 50 m (v_{10} and v_{50}); potential temperature (θ), equivalent potential temperature (θ_e) and temperature (T); all temperatures are measured at 2 m. The arrows indicate the positions of the front lines discussed in the text.

the small-scale flow did not change significantly during a period of one or two hours.

In summary, we point out that the structures of relative flow determined by rawinsondes, VAD radar data and Doppler mode radar scans give a consistent, though scale dependent picture: positive relative "feeder flow" in the meso-scale and bore-type features in the small-scale at the leading edge.

4.3.2. Surface observations. Let us now consider meteorological data taken at a 50 m tower situated in Garching. Time series of wind direction and wind speed at two different heights, and of equivalent potential, potential and dry air temperatures at 2 m are displayed in Fig. 14 for the period 06 to 15 GMT. The pre-frontal wind traces show wind velocities up to 2 m s^{-1} (at 10 m) and 5 m s^{-1} (at 50 m) towards the west which is typical for foehn situations in the Munich area when the surface-based cold air is not removed. Also the radar data (Fig. 6) show a low-level pre-frontal flow of $(u-c)$ equal to -25 m s^{-1} which is equivalent to an absolute flow of about 7 m s^{-1} towards the west. About 30 min in advance of the passage of the cold front, the wind direction veered towards the south-west with decreasing wind speeds. A sudden gust and a veering of wind direction to westerly (at the 10 m height) and to north-westerly (at the 50 m height) indicate the passage of the front line.

However, the frontal passage is not marked in the temperature traces. The gradual change in air mass can be recognized only in the humidity field, here expressed by equivalent potential temperature, which exhibited a decrease of 9 K within less than 1 h. This decrease commenced 1 h after the discontinuity in wind and pressure (Fig. 14). As mentioned above, there was a significant temperature drop of about 5 K at 1100 and 1400 m MSL associated with the passage of the cold front (Fig. 9). A similar change in temperature was observed when the aircraft took off in Oberpfaffenhofen in the surface-based cool air and rose into the warm air in the foehn region aloft (temperature increase by 5 K; relative humidity drop from 90% to 40%). This temperature difference is similar in magnitude to the difference between the pre-frontal warm foehn air and the post-frontal cold air. Therefore, a change in air mass was not apparent in the surface temperature at a place where the foehn did not touch the ground. If we extrapolate from the time series to horizontal surface distributions of pressure, wind, temperature and humidity, we conclude that a frontal line, which is characterized by a pressure jump and a sudden gust with wind shift, preceded the airmass boundary (marked by a drop in equivalent potential temperatures) by 1 h or 60 km. The former coincides with the disturbance marked by the roll clouds, the latter represents the surface front as it would be analysed on a synoptic chart.

Time series of pressure deviations from an arbitrary mean, measured by sensitive digital barometers, are shown in Fig. 15 for the stations Garching, Oberpfaffenhofen, Wielenbach, Uffing, and Thalreit. Common features are a continuous decrease during the morning hours, followed by 3 stages of pressure increase: steady rise (period AB), sudden jump (period BC) and further rise. Durations of periods AB and BC and the respective magnitudes of pressure rise are summarized in Table 1. These data are aug-

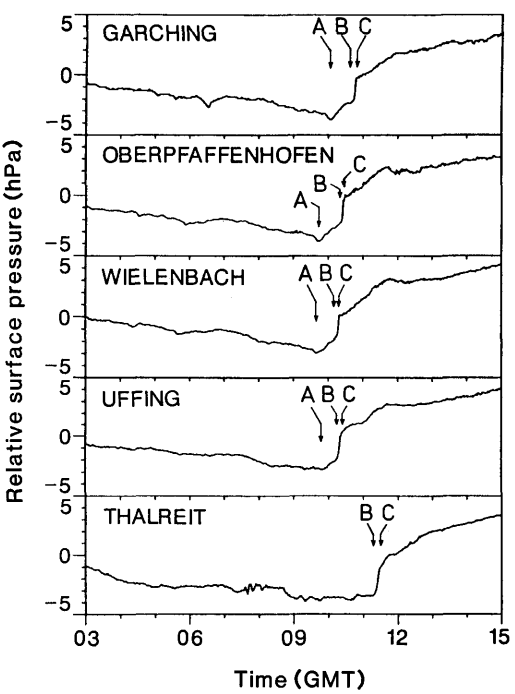

Fig. 15. Temporal evolution of surface pressures relative to an arbitrary mean at 5 stations. Indicated times A, B and C are detailed in Table 1.

Table 1. *Details of pressure jumps (see Fig. 15); Δx: distance to Alpine baseline; the times are given in GMT*

		Times/Pressure differences		
		A	B	C
Location	Δx (km)	Δt (min) Δp (hPa)	Δt (min) Δp (hPa)	
		1006	1044	1048
Garching (GA)	55	38 1.7	4 1.8	
		0946	1023	1029
Oberpfaffenhofen (OP)	46	37 1.7	6 2.2	
		0940	1016	1019
Wielenbach (WI)	30	36 1.5	3 1.5	
		0953	1017	1023
Uffing (UF)	12	24 1.1	6 1.9	
		—	1118	1128
Thalreit (TH)	3	— —	10 2.2	
		1000	1035	1038
Mühldorf (MD)	50	35 0.7	3 1.6	

mented by readings from a microbarograph located in Mühldorf where a similar temporal evolution was observed as in Garching and Oberpfaffenhofen.

The magnitude of the pressure jumps (BC), which are synchronous with the passage of the roll clouds, increase with decreasing distance from the Alpine baseline. The magnitudes are similar to the ones observed with cold air outflows from thunderstorms (Wakimoto, 1982). They are primarily hydrostatic, as can be estimated by a comparison of the jump in Thalreit and temperature soundings prior to and after the passage of the disturbance (see below and Fig. 18).

Significant is the fact that the duration of period AB was shorter the closer the station lies to the Alpine baseline; at a distance of about 50 km in Garching and Mühldorf it lasted about 40 min, whereas the jump came directly from the minimum value in Thalreit (3 km). Furthermore, a comparison between the values observed in Garching and Oberpfaffenhofen with those from Mühldorf some 50 km to the east yields a decrease in magnitude which suggests a dissipation of the observed structure towards the east.

Of particular interest is that the rise in pressure occurs before the arrival of the cold air (AB) at locations not too close to the Alps. An attempt is made to explain the apparent differences looking at time–height cross-sections of the virtual potential temperature, θ_v (Fig. 16), above Munich (55 km off the Alpine baseline) and Thalreit (at the baseline). This quantity is defined by

$$\theta_v = \theta\left(1 + \frac{R_d}{R_v} q\right),$$

with the gas constants for dry and humid air, $R_d = 287.1\ \mathrm{J\,kg^{-1}\,K^{-1}}$ and $R_v = 461.5\ \mathrm{J\,kg^{-1}\,K^{-1}}$, respectively, and the specific humidity q. It equals the potential temperature of a dry air mass of the same density, and therefore serves as a measure for weight of moist air.

Let us concentrate on the period between 09 GMT and the passage of the surface front lines (arrows, Fig. 16) which is characterized by the leading edge of the cold air. The surface front crossed Munich (Thalreit) shortly after 10 (11)

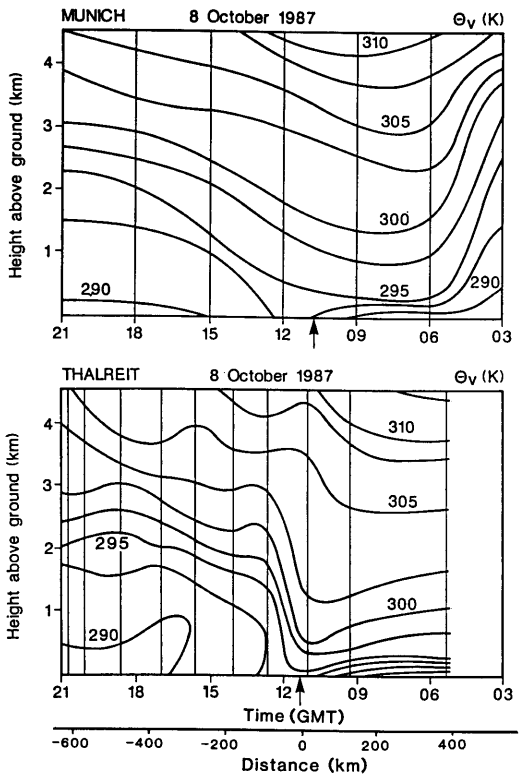

Fig. 16. Time–height cross-section of virtual potential temperatures θ_v above Munich (top) and Thalreit (bottom) on 8 October 1987. The passages of the surface front lines are indicated by arrows.

GMT. But at both stations the temperature started to decrease already one or two hours earlier at heights above 3 km. It seems that the upper air cold front preceded the surface front line. Below a height of 3 km the temperatures over Munich and Thalreit behave quite different prior to the passage of the surface front line. Over Munich the temperature decreased also, but increased over Thalreit due to the pre-frontal foehn. The pre-frontal low- to mid-tropospheric cold air advection over Munich may explain the increase of surface pressure ahead of the surface front line. Over Thalreit, i.e., close to the Alps, the effects of the warming near the ground and cooling aloft compensate and thus in turn the surface pressure traces show no increase of pressure in advance of the surface front line; the pressure just starts rising with the arrival of the cold air at the surface.

But caution is necessary: the temporal resolution of radiosoundings does not account for small-scale features. The observed pressure rises at label A are presumably accompanied by pre-frontal discontinuities of θ_v somewhere aloft. However, the short length of the period AB (40 min at most) makes it difficult to relate pressure trace characteristics to features aloft, which were analysed from rawinsondes launched at interval of 3 h (Munich) and 1.5 h (Thalreit). In summary, one must say that we can only hypothesize about the cause for the observed pressure traces, since the temporal resolution of the upper air data is not sufficient for firm conclusions.

From Fig. 16, it is also interesting to note that the cross-frontal gradients in θ_v are much stronger in the vicinity of the Alps than above Munich 50 km to the north of the baseline. The maximum gradients above Munich are about 4 K per 50 km whereas above Thalreit values up to 7 K per 50 km occurred. If we assume that the cross-frontal gradients in temperature had no along-front variations over, say, France where the front was not influenced by the Alps, the above mentioned gradients suggest that the orography increases the strength of the frontal line by strengthening the cross-frontal pressure and temperature gradients. This implies that the barrier exerts a frontogenetic influence on the front.

In Ulm, the pressure trace is quite different (Fig. 17a). Two short periods of increase are separated by about 3 min of decrease, leading to a wave-like appearance. After 10 min of constant pressure a further increase is observed. The registration of rain-rates reveals two distinct precipitation maxima, the first between 0850 and 0910 GMT and the second between 0920 and 0950 GMT, with a gap of significantly reduced precipitation in between (Fig. 17b). It is interesting to note that the precipitation started during the pressure drop shortly after the first peak in pressure. This is similar to the observations discussed by Parsons et al. (1987) who pointed out that the pressure rise at the leading edge leads the main precipitation by a few minutes. The temporal structure of the rainrates suggests that the first maximum is associated with a narrow frontal rainband followed by a wider rainband. However, a banded structure of the precipitation cannot be derived without doubts from Fig. 10.

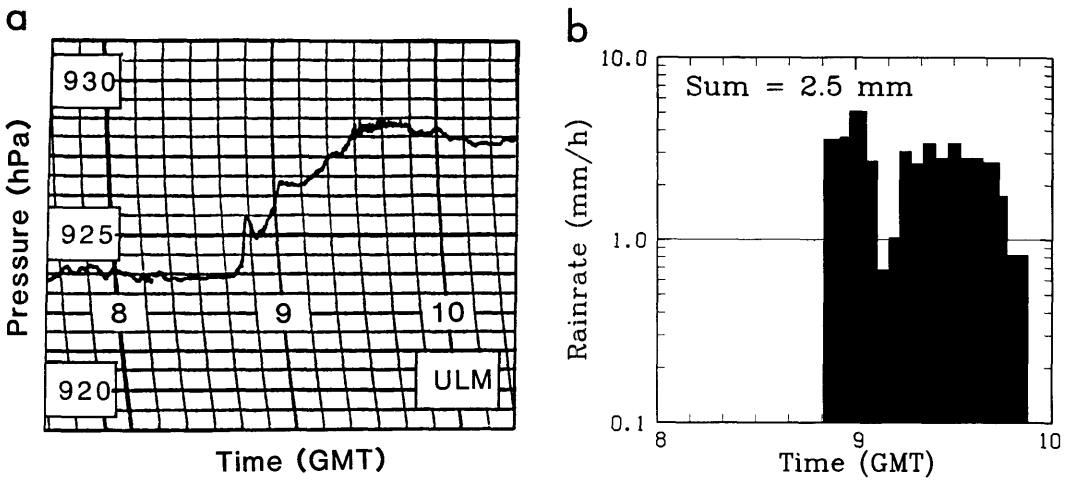

Fig. 17. Pressure trace (a) and precipitation rates (b) between 08 and 10 GMT as measured in Ulm.

Altogether, all pressure traces from the area east of Ulm, where no precipitation was recorded, exhibit the jump as a distinct feature. We note that the short-period differences between single stations are significantly smaller than those in a collection of synchronous pressure traces observed during the Australian cold fronts research programme (Garratt et al., 1985).

4.3.3. Aircraft observations. When the roll clouds had passed Oberpfaffenhofen, a powered glider (PG3 in Fig. 1) took off to chase the disturbance. It succeeded in making a circumference flight in the vicinity of the Chiemsee, a lake situated 10 km off the Alpine baseline. In Fig. 18, the soundings just prior to and after the roll cloud are compared with a pre-/post-frontal pair of ascents from the nearby rawinsonde station Thalreit. The pre-frontal soundings agree well; they show a low-level stable layer topped by a neutral layer above 800 hPa. The post-frontal data display a well mixed, neutral boundary layer underneath a stable stratification. The Thalreit ascent is systematically colder by about 2 K as it was measured 80 km behind the leading edge of the front, whereas the sailplane sounding took place only 10 km behind it. As already mentioned, we note that the observed rise in surface pressure between the two soundings in Thalreit ($\Delta p = 5$ hPa) is of similar magnitude as the calculated hydrostatic pressure increase (6 hPa) due to the observed 6 K decrease of the vertically averaged potential temperature.

In order to obtain a combined picture of the airflow and temperature fields in a frame of reference moving with the surface front line, a composite diagram (Fig. 19) is constructed from the velocity measurements obtained by the Doppler radar at Oberpfaffenhofen (1023 GMT; see left portion of Fig. 13) and the temperature obtained by the Queenair near Bad Tölz (1050 GMT; see Fig. 9) and by a powered glider (PG3 in Fig. 1) in the vicinity of Chiemsee (1122 to 1218 GMT). In a first approach, we assume that

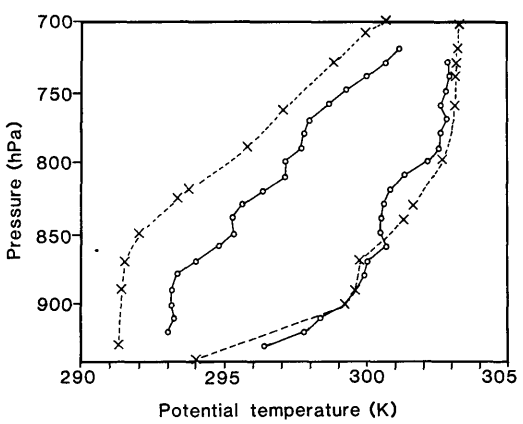

Fig. 18. Soundings before (right) and after (left) the passage of the roll cloud on 8 October 1987. The crosses stand for the soundings in Thalreit (before: 1059 GMT; after: 1236 GMT, approx. 80 km behind the roll); the circles designate the soundings measured by powered glider (PG3 in Fig. 1) in the vicinity of Chiemsee (before: 1139 GMT; after: 1206 GMT, approx. 10 km behind the roll).

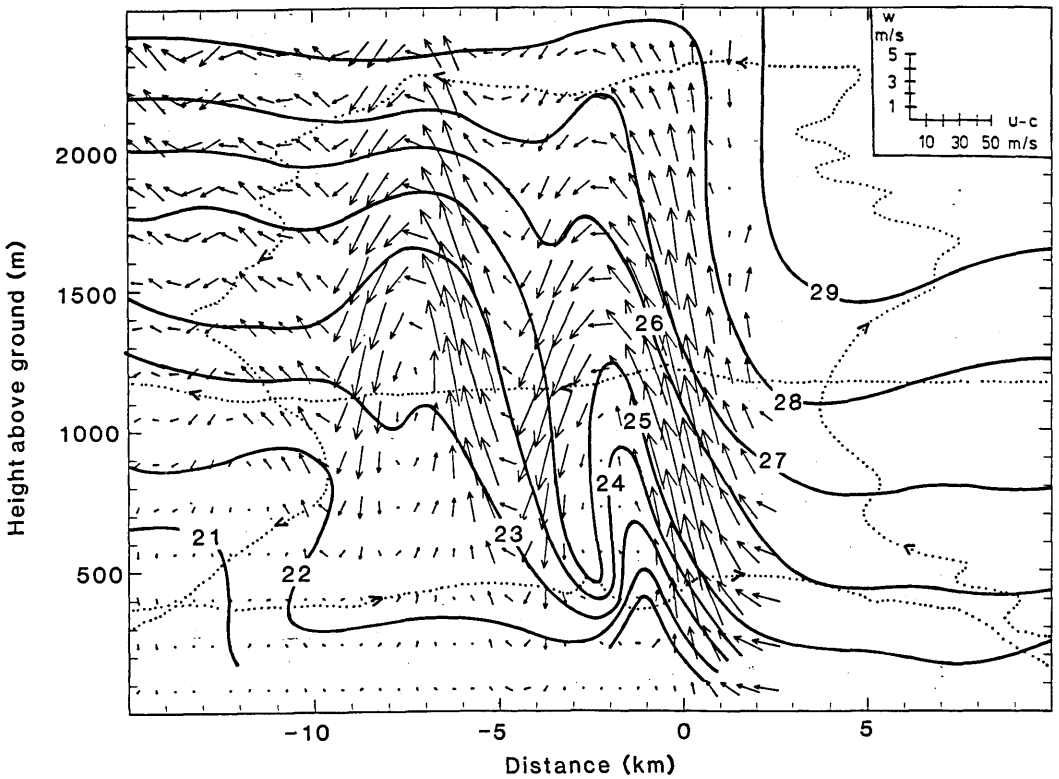

Fig. 19. Composite of airflow and potential temperature (°C) in a frame of reference moving with the surface front line (at 0 km) as determined by the Doppler radar in Oberpfaffenhofen and aircraft (flight tracks dotted; Queenair in the middle; circumference flight by powered glider PG3). See text for details. The scale of the horizontal and vertical wind is given in the top right corner.

the main characteristics of the leading edge of the front remained unchanged for about 1 h which is reasonable as discussed above. The differences in time and space between the temperature and the wind fields depicted in Fig. 13 are about 1 h and 100 km, respectively. Additionally, we keep in mind that the temperature field was obtained 10 to 15 km off the Alpine baseline, whereas the wind field was observed 50 km to the north of it.

The cross-frontal temperature gradients at the leading edge are about 3 K km^{-1} over a distance of 2 km. Comparable small-scale gradients measured by aircraft are 4 K km^{-1} across a front in New Mexico (Shapiro et al., 1985) and 8 K km^{-1} over the ocean (Bond and Fleagle, 1985). During a very strong cold front in Colorado 3 K per 100 m were encountered by high-resolution tower measurements (Shapiro et al., 1985). Our composite diagram shows that the waves in the airflow coincide partly with an up and down pattern in the θ field. In the leading updraught the flow is parallel to the isentropes whereas further to the west this is not the case. The flow is parallel to the isentropes when it is stationary, frictionless and two-dimensional. In the present case the flow is not parallel to the isentropes and it cannot be decided whether the discrepancy is due to non-stationarity, due to the presence of friction in a three-dimensional flow, or due to inevitable uncertainties in the positioning of the temperature data. But it is obvious that the wavelength of the temperature (L_θ) and of the velocity disturbance (L_u) are different: $L_\theta = 2.8$ km and $L_u = 4.8$ km.

The temperature data taken by the Queenair along the flight track indicated in Fig. 19 at a height of 1200 m above ground were collected at about 1050 GMT and approximately 80 km to

the west from those temperature data collected during the circumferential flight around 1200 GMT by the powered glider. Both data sets show similar L_θ and even the temperature wave observed by powered glider PG1 earlier at 0944 GMT some 90 km further to the west (Fig. 9, top) has a similar wavelength. Thus, it is possible that during the time between 09 and 12 GMT the temperature structure did not change, in particular close to and parallel to the Alps. The wind measurements were taken in the middle of the period in question at 1023 GMT, but 50 km to the north of the baseline. Therefore, it is suggestive to state that the difference in wavelength in the temperature and wind field depends on the distance to the barrier.

An important point is the determination of the precise aircraft positions, from which the relative position from the surface front can be calculated. These positions are constructed using a number of time marks at the passages of the cloud line and other fixed locations and the registered headings and air speeds of the aircraft combined with the assumption of a constant wind in between. Taking into account these uncertainties, the differences in the wavelengths remain significant. This indicates, in our view, that the dependency of the wavelength on the distance to the barrier is a real feature of an orographically influenced flow.

5. Discussion and summary

Three different topics appear quite naturally when one tries to discuss and summarize the entire observational evidence: (a) the frontal circulation and its scale dependent aspects, (b) the gravity current features at the leding edge, and (c) the orographic impact on the front. These are dealt with in sequence.

5.1. Synthesis of the frontal circulation

The synoptic scale features of the front have the characteristics of a cold front of the ana-type (Fig. 5) whereas in the small scale some features of a density current are evident (Fig. 13). It is interesting to note that our synoptic-scale pattern is very similar to the observed frontal pattern discussed by Browning and Harrold (1970). In contrast to our observations, they find as small-scale feature only one strong updraught at the leading edge of the front associated with heavy precipitation and a "feeder flow" from aloft with negative relative flow at the surface (Fig. 5 in their paper). This means that their front had a similar structure in the synoptic- and in the small-scale. The small-scale structure observed in our front shows typical features as they are observed on gust fronts (Klingle et al., 1987).

The difference in scale is about 50 to 1 if we compare the synoptic- and the small-scale circulation patterns in their temporal and horizontal scales. The horizontal extension of the synoptic-scale circulation shown in Fig. 5 is about 1000 km or 1000 min versus 20 km and 20 min shown in Fig. 13. The question remains how both circulations are related to each other? A possible explanation for the observations in this case is schematically drafted in Fig. 20. At the low-level leading edge of the synoptic-scale ana-front, a shallow gravity current has probably evolved in southern Germany. Its modification during its eastward propagation is discussed in Subsection 5.2.

The next question remains: what were the causes for the generation of this gravity current? We can only give a speculative answer. After the cold front had crossed the Rhine River at 07 GMT it was accompanied by moderate to strong precipitation. The accumulated precipitation was between 3 and 9 mm during the period between 06 and 12 GMT on 8 October 1987. Fig. 17 shows the precipitation rate at Ulm close to the eastern edge of the area with precipitation (cf. Fig. 10). Between 09 and 10 GMT the rates reached up to 5 mm h^{-1}. The area with precipitation was limited to the east by a line from the

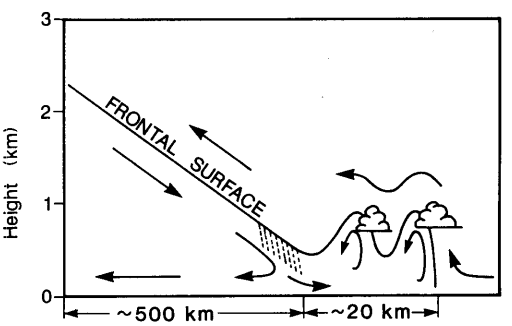

Fig. 20. Schematic representation of the large- and small-scale features of the front of 8 October 1987. The arrows indicate the streamlines relative to the moving system.

Lake of Constance towards some 30 km to the east of Ulm and from there towards the north-east; to the east of this area the foehn was blowing. The three roll clouds were observed in a region bounded to the south by the Alpine baseline and to the west by the area with precipitation.

Two different aspects may have influenced the front when it approached the foehn influenced region. Firstly, the pre-frontal moist low-level jet, often called warm conveyer belt, was cut off and replaced by very dry warm foehn air. Therefore, the advection of moist air was significantly reduced and in turn the precipitation stopped as is apparent in the radar data (Fig. 10). The cut-off of moist air is simulated in a recent numerical study using a meso-scale model (Majewski, 1988), which compared simulations of the front of 8 October 1987 including the Alps with runs where the Alpine orography was replaced by a 500 m high plateau above mean sea level. In the plateau case, the frontal precipitation moved undisturbed from west to east, whereas in the case with Alps the precipitation ceased in the area of Ulm and the eastern regions received no precipitation as time progressed.

Secondly, the pre-frontal air was significantly warmer due to the foehn, so that the cross-frontal temperature gradient increased. It is possible that there was a further increase of the cross-frontal temperature gradient due to evaporative cooling in the precipitation area, producing a cold pool. This cold pool spreads under its own weight as a gravity current, propagating ahead of the triggering front as a shallow outflow (Seitter and Muench, 1985). Measurements of such passages of sharp frontal lines ahead of the major frontal system have given rise to the process suggested in Fig. 20. When the vertical humidity structure is close to saturation, hence, in case of lifting, roll clouds or "rope clouds" as some authors call them appear (Seitter and Muench, 1985).

In general, the environmental conditions of the dry pre-frontal foehn air and the cold post-frontal air probably due to evaporation were favourable for generating a circulation in which roll clouds developed.

5.2. *Gravity current features*

A gravity current is characterized by a low-level flow towards the nose feeding the head whereas above the head the relative flow is backwards (Schmidt, 1911). Some of the small-scale features of the leading edge of the front of 8 October 1987 are similar to those of a gravity current, especially the positive relative flow near the ground (Fig. 13) and the sudden pressure jumps (Fig. 15). The alternating signs in the relative velocity components (Fig. 13) and the appearance of roll clouds, however, indicate that the gravity current must have undergone a distinct transformation on its way from its probable source region in the west of southern Germany. We assume that these bore-like features are a consequence of the gravity current's interaction with the shallow, ground based stable layer, which existed over the eastern part of southern Germany due to south foehn. Such a view is backed by results from numerical experiments where an initially pure gravity current was run into a stably stratified environment and bore-like flow structures evolved (Haase and Smith, 1989).

An idea, which seems to have validity in some regions with high mountain barriers, is that the component of flow normal to the ridge in the cold air is blocked and surges along the barrier as a gravity current with the latter to its right (in the northern hemisphere). If geostrophic balance exists normal to the mountain range, theory shows that the surge would be confined to within a deformation (Rossby) radius of the barrier by the Coriolis force. This means that the along mountain velocity component is determined geostrophically by the pressure gradient normal to the barrier. The Rossby radius of deformation is given by

$$D = (g' h)^{1/2}/f,$$

with h the height of the front, g' the reduced gravity, $g' = g\Delta\theta/\theta$, $\Delta\theta$ a characteristic potential temperature difference between the warm and cold air, θ the potential temperature of the cold air, and g the acceleration due to gravity. HS88 estimated the Rossby radius using Baines' (1980) simple theory and obtained a value of about 250 km using a cross-frontal temperature gradient of 9 K derived from the soundings at Thalreit. Aircraft data suggest a weaker cross-frontal temperature contrast of only 7 K, however, within a shorter distance; this leads to a radius of deformation of 220 km. Thus, to the extent that this simple theory is applicable, we conclude that any

deformation of the surface front caused by a surge would have been detectable by the station network. As indicated by the isochrones for this event (see HS88, their Fig. 4) this was not the case. However, considering the surface pressure distribution at 12 GMT (Fig. 21) we see that the isobars are parallel to the surface front line at its rear side within a distance of about 60 km and that the wind directions are normal to the isobars. This indicates a significant ageostrophic cross-isobaric mass flux within the distance of the above computed Rossby radius. Further to the north the ageostrophy is much weaker (not shown).

In the case of a steady gravity current the speed c of the current is directly related to the cross-frontal density gradient expressed by $\Delta\theta: c = (g' h)^{1/2}$. It seems to be reasonable to apply this simple theory to our case with the values $\theta = 290$ K, $\Delta\theta = 7$ K from the temperature trace taken by the Queenair at 1400 m MSL (Fig. 9), and $h = 2000$ m. We obtain a speed of the current of 21.8 m s^{-1}. This value is of the same order of magnitude as the observed speeds between 18 and 20 m s^{-1}. However, one has to keep in mind that small changes in the chosen values of h, θ and $\Delta\theta$ may change the result dramatically. Therefore the main problem in applying the speed formula is the selection of the input data which are characterized by a considerable error range in realistic flow situations. This shows that this simple theory is not particularly meaningful in our case, either because it was not a steady situation or because the approach is too simple. So, we conclude that the speed equation of gravity current is of questionable relevance for the application to real fronts as pointed out by Smith and Reeder (1988).

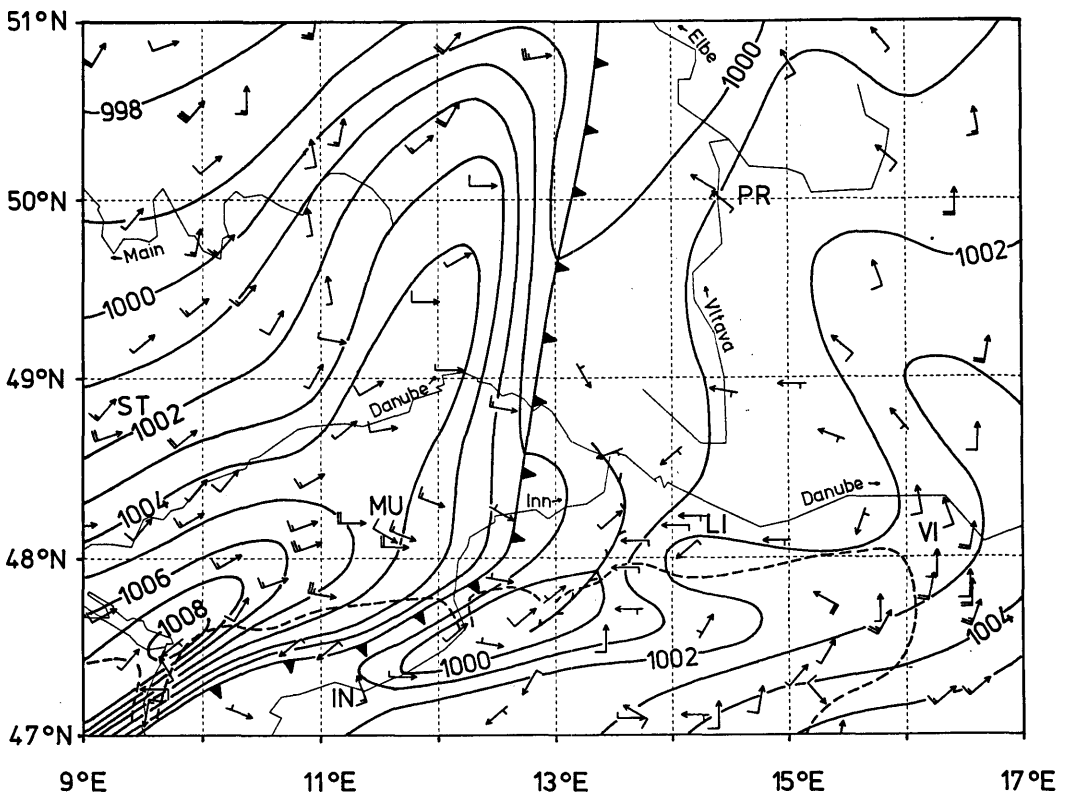

Fig. 21. Mesoscale surface analysis for 8 October 1987, 12 GMT showing the surface front line and a preceding convergence line; wind speed in knots (standard notation); pressure in hPa; the Alpine baseline is dashed; locations: Linz (LI), Innsbruck (IN), Munich (MU), Prague (PR), Stuttgart (ST) and Vienna (VI).

5.3. The orographic impact

The interaction of the pre-frontal foehn with the precipitating cold front was an important aspect of the front of 8 October 1987. The observations indicate that the Alps induced an approximately 80 km wide belt without precipitation to the north of their baseline, in which the cold front progressed eastwards as a dry disturbance. This effect was also shown by Majewski (1988), who discussed a numerical simulation of this frontal event.

Fig. 21 reveals that the low-level flow was significantly blocked at the north-western edge of the Alps close to the Lake of Constance. The magnitude of the resulting meso-scale high increased from 1005 hPa to 1008 hPa as the front approached the Alps between 06 and 12 GMT on 8 October 1987. As the front moved towards the east in the afternoon the maximum pressure further increased to 1010 hPa; however, it remained in the same position at the north-western flank of the Alps. A similar blocking effect was reported by Heimann and Volkert (1988) during another frontal event in that area. An important feature is the pre-frontal meso-scale low induced by the pre-frontal foehn. The basic surface pressure distribution during foehn is characterized by a ridge of high pressure at the windward side of the Alps and a meso-scale lee trough (Hoinka and Rösler, 1987). This lee trough, apparent in Fig. 21, is deformed by the approaching front and hence an increase in the cross-frontal gradients in surface pressure occurs as the front progresses towards the east along the northern side of the Alps. At the eastern edge of the Alps a surface flow around them from the south is apparent, which turns into an easterly flow just north of the Alpine baseline. This is typical for a south-foehn situation.

The main results concerning the impact which the Alps most probably exerted on the front of 8 October 1987 are summarized as follows.

- There is evidence that the magnitude of the pressure jump associated with the leading edge of the front is stronger in the vicinity of the Alps than at a greater distance from the orography.
- The cross-frontal gradients in θ_v are significantly stronger above the Alpine baseline than above Munich 50 km to the north of it.
- The wavelength associated with the up- and down-draughts just behind the leading edge of the front is smaller close to the Alps than further to the north.
- The synoptic-scale circulation characteristic for ana-type fronts with a "feeder flow" from aloft in the rear of the front exists at a distance of 50 km north of the Alps, whereas it disappears close to the Alps.
- Due to the presence of a surface-based cold air during pre-frontal foehn situations there is no temperature drop associated with the passage of the front at the surface in the area around Munich in contrast to locations closer to the Alps where the foehn has eroded the cold air.
- The occurrence of a shallow-layer disturbance made visible by the roll clouds between the baseline of the Alps and the Danube River seems to be a side-effect of the orography; the possible influence is that both the frontal precipitation and the pre-frontal foehn, which dried out the pre-frontal atmosphere, have generated a preferable environment to produce these roll clouds.
- The low-level part of the front was retarded by the Alps on their western edges, whereas the upper level front crossed the Alps without being distorted; the blocking effect of the mountains is clearly evident as the cold front arrived in Innsbruck at about 1700 GMT, at the same time that it reached Vienna some 400 km to the east; Innsbruck is separated from the (relative) plain of southern Bavaria by the Karwendel mountains which have a mean height of 2000 m; this ridge blocked the southward progression of the cold air which arrived in Innsbruck from the east along the Inn Valley.

Some of the above-mentioned facts suggest that the orography can increase the cross-frontal temperature gradients via the orographically generated pre-frontal foehn and due to the low-level blocking of the cold air.

In conclusion, we think that the front of 8 October 1987 was an important event revealing small- to synoptic-scale features of a front which became considerably influenced by the Alps in general and by pre-frontal foehn in particular. It is hoped that the analyses of other events probed during the German Front Experiment 1987 will

result in providing further details concerning the influence of the Alps on cold fronts and, thus, will help to verify or disprove the conjectures on the orographic impact presented above.

6. Acknowledgements

We wish to record our thanks to all the colleagues who participated in the German Front Experiment 1987. In particular, we thank the German Weather Services for the supply of data including the additional rawinsonde soundings, which were funded by a grant from the German Science Foundation (DFG) under the title "fronts and orography". We are especially grateful to Manfred Kurz (DWD) for providing the synoptic-scale frontal analysis. Roger K. Smith (University Munich) is thanked for initiating the flight around the leading edge of the roll cloud and commenting on an earlier version of the paper. Special thanks for the provision of data are due to: Hans Müller (FhG, Garmisch), pressure data; Heinz Lößlein (University Munich), surface data from Garching; Frank Rösler (DLR, Oberpfaffenhofen), Queenair data; Hermann Willeke (DLR), powered glider data; Heinz Löbel (DLR), Thalreit rawinsonde data; Klaus-Peter Schickel (DLR), NOAA images. The attempt to define the various aspects of the term "front" stems from a discussion with Reinhold Steinacker (University Innsbruck), Veronica Zwatz-Meise and Christian Kress (both Zentralanstalt für Meteorologie und Geodynamik, Vienna). An anonymous reviewer and Melvin A. Shapiro are acknowledged for their critical reviews and helpful comments.

REFERENCES

Baines, P. G. 1980. The dynamics of the southerly buster. *Aust. Meteor. Mag. 28*, 175–200.

Bond N. A. and Fleagle, R. G. 1985. Structure of a cold front over the ocean. *Quart. J. R. Met. Soc. 111*, 739–759.

Browning, K. A. and Harrold, T. W. 1970. Air motion and precipitation growth at a cold front. *Quart. J. R. Met. Soc. 96*, 369–389.

Browning, K. A. and Wexler, R. 1968. The determination of kinematic properties of a wind field using Doppler radar. *J. Appl. Meteor. 8*, 105–113.

Carbone, R. E. 1982. A severe frontal rainband. Part I: Stormwide hydrodynamic structure. *J. Atmos. Sci. 39*, 258–279.

Chromow, S. P. 1940. Einführung in die synoptische Wetteranalyse (in German; Introduction to synoptic-scale weather analysis). Vienna: Springer, 532 pp.

Colquhoun, J. R., Shepherd, D. J., Coulman, C. E., Smith, R. K. and McInnes, K. 1985. The southerly burster of southeastern Australia: an orographically forced cold front. *Mon. Wea. Rev. 113*, 2090–2107.

Cook, A. W. and Topil, A. G. 1952. Some examples of chinooks east of the mountains in Colorado. *Bull. Amer. Meteor. Soc. 33*, 42–47.

Coulman, C. E., Colquhoun, J. R., Smith, R. K. and McInnes, K. 1985. Orographically forced cold fronts—mean structure and motion. *Bound. Lay. Meteor. 32*, 1478–1486.

Garratt, J. R., Physick, W. L., Smith, R. K. and Troup, A. J. 1985. The Australian summertime cool change. Part II: Mesoscale aspects. *Mon. Wea. Rev. 113*, 202–223.

Haase, S. P. and Smith, R. K. 1989. The numerical simulation of atmospheric gravity currents. Part II: Environments with stable layers. *Geo. Astro. Fluid Dyn. 46*, 35–51.

Heimann, D. and Volkert, H. 1988. The "papal front" of 3 May 1987—mesoscale analyses of routine data. *Beitr. Phys. Atmosph. 61*, 62–68.

Hobbs, P. V. and Persson, P. O. G. 1982. The mesoscale and microscale structure and organization of clouds and precipitation in midlatitude cyclones. Part V: The substructure of narrow cold-frontal rainbands. *J. Atmos. Sci. 39*, 280–295.

Hoinka, K. P. 1985. On fronts in central Europe. *Beitr. Phys. Atmosph. 58*, 560–571.

Hoinka, K. P., Fimpel, H. P. and Köpp, F. 1988. An intercomparison of meteorological data taken by aircraft, radiosondes and a laser-Doppler-anemometer. *Theor. Appl. Climatol. 39*, 30–39.

Hoinka, K. P. and Rösler, F. 1987. The surface layer on the leeside of the Alps during foehn. *Meteorol. Atmos. Phys. 37*, 245–258.

Hoinka, K. P. and Smith, R. K. 1988. A dry cold-front over southern Bavaria. *Weather 43*, 255–261.

Hoinka, K. P. and Volkert, H. 1987. The German Front Experiment 1987. *Bull. Amer. Meteor. Soc. 68*, 1424–1427.

Klingle, D. L., Smith, D. R. and Wolfson, M. W. 1987. Gust front characteristics as detected by Doppler radar. *Mon. Wea. Rev. 115*, 905–918.

Majewski, D. 1988. Die Front vom 8.10.87 simuliert mit dem Europa-Modell des Deutschen Wetterdienstes (in German; The front of 8 October 1987, simulated with the "Europe-Model" of the Deutscher Wetterdienst). *DWD-intern Nr. 20*, Offenbach, 70 pp. (Available from: Deutscher Wetterdienst, Abteilung F, Frankfurter Straße 135, D-6050 Offenbach, FRG.)

Mass, C. F. and Albright, M. D. 1987. Coastal southerlies and along-shore surges of the west coast of North America: evidence of mesoscale topographically trapped response to synoptic forcing. *Mon. Wea. Rev. 115*, 1707–1738.

Orlanski, I. 1975. A rational subdivision of scales for atmospheric processes. *Bull. Amer. Meteor. Soc. 56*, 527–530.

Parsons, D. B., Mohr, C. G. and Gal-Chen, T. 1987. A severe frontal rainband. Part III: Derived thermodynamic structure. *J. Atmos. Sci. 44*, 1615–1631.

Passarelli, R. E., Romanik, P., Geotis, S. G. and Siggia, A. D. 1981. Ground clutter rejection in the frequency domain. Preprints of the 20th Conference on Radar Meteorology, Boston. Boston: American Meteorological Society, 295–300.

Schmidt, W. 1911. Zur Mechanik der Böen (in German; On the mechanics of gusts). *Z. Meteorol. 28*, 355–362.

Schroth, A., Chandra, M. and Meischner, P. 1988. A C-band coherent polarimetric radar for propagation and cloud physics research. *J. Atmos. Ocean. Techn. 5*, 803–822.

Seitter, K. L. and Muench, H. S. 1985. Observation of a cold front with rope cloud. *Mon. Wea. Rev. 113*, 840–848.

Shapiro, M. A., Hampel, T., Rotzoll, D. and Mosher, F. 1985. The frontal hydraulic head: a micro-α scale triggering mechanism for mesoconvective weather systems. *Mon. Wea. Rev. 113*, 1166–1183.

Smith, R. K. and Morton, B. R. 1984. An observational study of northeasterly 'morning glory' wind surges. *Aust. Met. Mag. 32*, 155–175.

Smith, R. K. and Reeder, M. J. 1988. On the movement and low-level structure of cold fronts. *Mon. Wea. Rev. 116*, 1927–1944.

Wakimoto, R. M. 1982. The life cycle of thunderstorm gust fronts as viewed with Doppler radar and rawinsonde data. *Mon. Wea. Rev. 110*, 1060–1082.

Zwatz-Meise, V. 1987. Satellitenmeteorologie (in German; Satellite meteorology). Verständliche Wissenschaft Band 17. Berlin: Springer Verlag, 169 pp.

Zwatz-Meise, V. and Kress, Ch. 1988. Frontexperiment 1987: 7–8 October, diagnosis with satellite images and derived meteorological parameters. DFVLR Frontexperiment—Note No. 12, 38 pp. (Available from the authors, Zentralanstalt für Meteorologie und Geodynamik, Hohe Warte 38, A-1191 Wien, Austria.)